CAPS1 Regulates Catecholamine Loading of Large Dense-Core Vesicles

Dina Speidel,[1,7] Cathrin E. Bruederle,[2,7]
Carsten Enk,[1] Thomas Voets,[3,8]
Frederique Varoqueaux,[1] Kerstin Reim,[1]
Ute Becherer,[2] Francesco Fornai,[4,5]
Stefano Ruggieri,[5] Yvonne Holighaus,[6]
Eberhard Weihe,[6] Dieter Bruns,[2] Nils Brose,[1,*]
and Jens Rettig[2,*]

[1]Max-Planck-Institut für Experimentelle Medizin
Abteilung Molekulare Neurobiologie
D-37075 Göttingen
Germany
[2]Universität des Saarlandes
Physiologisches Institut
D-66421 Homburg/Saar
Germany
[3]Max-Planck-Institut für Biophysikalische Chemie
Abteilung Membranbiophysik
D-37077 Göttingen
Germany
[4]University of Pisa
Department of Human Morphology
  and Applied Biology
I-56126 Pisa
Italy
[5]Laboratory of Neurobiology of Movement Disorders
IRCCS Neuromed
I-86077 Pozzilli (Isernia)
Italy
[6]Philipps-Universität Marburg
Institut für Anatomie und Zellbiologie
Abteilung Molekulare Neurowissenschaften
D-35033 Marburg
Germany

Summary

CAPS1 is thought to play an essential role in mediating exocytosis from large dense-core vesicles (LDCVs). We generated CAPS1-deficient (KO) mice and studied exocytosis in a model system for Ca^{2+}-dependent LDCV secretion, the adrenal chromaffin cell. Adult heterozygous CAPS1 KO cells display a gene dosage-dependent decrease of CAPS1 expression and a concomitant reduction in the number of docked vesicles and secretion. Embryonic homozygous CAPS1 KO cells show a strong reduction in the frequency of amperometrically detectable release events of transmitter-filled vesicles, while the total number of fusing vesicles, as judged by capacitance recordings or total internal reflection microscopy, remains unchanged. We conclude that CAPS1 is re-

quired for an essential step in the uptake or storage of catecholamines in LDCVs.

Introduction

Regulated secretion of neurotransmitters, hormones, or peptides is mediated by the Ca^{2+}-dependent fusion of secretory vesicles with the plasma membrane. Different types of secretory vesicles, small clear vesicles (SCVs) and large dense-core vesicles (LDCVs), are responsible for the secretion of classical neurotransmitters and peptides/neuromodulators, respectively. SCVs and LDCVs employ a very similar set of proteins for the regulation and execution of their Ca^{2+}-triggered fusion with the plasma membrane. Reflecting these molecular similarities, the final phases of SCV and LDCV exocytosis are characterized by the same basic vesicle trafficking steps. Vesicles are first tethered at the plasma membrane and then primed to fusion competence. Only primed vesicles, representing the "readily releasable vesicle pool," are able to fuse with the plasma membrane in response to rises in the intracellular Ca^{2+} concentration (Burgoyne and Morgan, 2003; Jahn et al., 2003; Rettig and Neher, 2002; Südhof, 1995).

Despite the fact that SCVs and LDCVs use similar proteins to control and execute membrane fusion, the two vesicle types differ in their morphology, lumenal and membrane protein complement, biogenesis, trafficking and recycling pathways, and release kinetics. Even at the level of common trafficking steps such as vesicle priming, differences in kinetics and regulatory mechanisms are apparent (Burgoyne and Morgan, 2003), but the molecular causes for these functional differences are unknown. Only very few proteins have been proposed to be specifically involved in the secretion of only one type of vesicle. One such protein is CAPS1, which is thought to be essential for LDCV but not SCV exocytosis (Ann et al., 1997; Berwin et al., 1998; Hay and Martin, 1992; Tandon et al., 1998; Walent et al., 1992).

CAPS1 is a 145 kDa protein that was discovered as an essential cytosolic factor in Ca^{2+}-triggered noradrenaline (NA) release from cracked PC12 cells, where it is required for a secretory step that follows ATP-dependent priming (Ann et al., 1997; Hay and Martin, 1992; Walent et al., 1992). It contains a central PH domain whose binding to acidic phospholipids is essential for CAPS1 function, an MH domain, which is also found in members of the Munc13 family of vesicle priming proteins, a C-terminal membrane association domain that mediates LDCV binding, and a core C$_2$ domain (Grishanin et al., 2002). Recently, a second CAPS isoform, CAPS2, was identified in mammals. CAPS2 is structurally and functionally similar to CAPS1 but exhibits a different cell/tissue and developmental expression pattern (Cisternas et al., 2003; Speidel et al., 2003). While CAPS1 expression is specific for neuronal and neuroendocrine tissues and the pancreas, CAPS2 is also found in other tissues (Speidel et al., 2003). Anti-

body inhibition studies in chromaffin cells (Elhamdani et al., 1999) and melanotrophs (Rupnik et al., 2000) indicated that CAPS1 is required for a late release phase of LDCV exocytosis, possibly by modulating fusion pore formation and dilation. Genetic studies on the invertebrate orthologs in *C. elegans* (Avery et al., 1993) and *Drosophila* (Renden et al., 2001) demonstrated that CAPS is an essential protein with an important role in the secretion of a subset of neurotransmitters. In *Drosophila*, deletion of CAPS causes a 50% decrease in glutamatergic transmission at neuromuscular junctions. However, this may be an indirect effect, as expression of CAPS in motor neurons does not rescue the phenotypic changes in neuromuscular junctions of CAPS mutants (Renden et al., 2001). Currently, CAPS1 is thought to act during the Ca^{2+}-triggering step of regulated LDCV exocytosis and/or fusion pore opening and dilation, but the corresponding evidence is not unequivocal. Published functional data are almost exclusively based on antibody inhibition studies, and genetic studies in *C. elegans* and *Drosophila* could not identify the LDCV trafficking step that is regulated by CAPS proteins.

To determine the function of CAPS1 in LDCV secretion, we generated and analyzed CAPS1-deficient mice (KOs).

Results

Characteristics of CAPS1 KOs

A KO mutation in the murine *CAPS1* gene was generated by homologous recombination in embryonic stem cells and detected as described in the Experimental Procedures (Figure 1A). Heterozygous CAPS1 KOs were viable and fertile and showed no obvious phenotypic alterations in the cage environment. Genotyping of offspring resulting from interbreeding of heterozygous mutants (Figures 1A and 1B) showed that at birth wild-type (wt; +/+), heterozygous KO (+/−), and homozygous KO (−/−) pups were present at the expected 1:2:1 Mendelian frequency (41:81:41). Western blot analysis of mutant brains showed that CAPS1 expression was abolished in homozygous KOs and significantly reduced to 44% ± 6% of wt levels in heterozygous KOs (Figure 1C). The expression of representative control proteins (Secretogranin 2, Synaptotagmin 1, Munc13-1, Munc18-1, and Syntaxin 1) was not altered (Figure 1D).

Newborn homozygous CAPS1 KO pups breathed slowly and moved only after tactile stimulation. After birth, breathing rates decreased, and mutant mice died within 10–30 min. Despite this perinatally lethal phenotype, homozygous CAPS1 KO mice showed no obvious changes of the body plan or individual organs (data not shown). Structure and cytoarchitecture of the brain and adrenal gland were indistinguishable from those seen in wt littermates (Figure 1F). Likewise, lung and heart of homozygous newborn CAPS1 KOs as well as the brain and adrenal gland of postnatal day 30 (P30) heterozygous KOs were histologically normal (Figure 1F and data not shown).

Western blot analyses of vesicular proteins essential for the filling of LDCVs with catecholamines in homogenates of adrenal glands from embryonic day 19 (E19) KO pups revealed expression levels of the vesicular H^+-ATPase (111% ± 7%), of the monoamine transporters VMAT1 (87% ± 6%) and VMAT2 (~85%), and of Chromogranin A (116% ± 9%) and CAPS2 (~104%) that were similar to wt levels (100%) (Figure 1E). Likewise, quantification of protein levels in adrenal homogenates from P30 heterozygous CAPS1 KOs revealed no changes in expression levels of vesicular proteins (data not shown). In contrast, CAPS1 expression was reduced to about 65% ± 6% in adrenals of adult heterozygous KO mice (Figure 1E). Immunohistochemical examination of VMAT1, VMAT2, and tyrosine hydroxylase (TH) in adrenal sections of E19 CAPS1 KO and wt adrenals revealed no differences between genotypes with respect to immunopositive cell numbers and staining intensity (Figure 1G).

Thus, CAPS1 is essential for postnatal survival of mice but not for the regulation of their development. Given the widespread expression of CAPS1 in neuronal and neuroendocrine tissues, possible reasons for the perinatally lethal phenotype of CAPS1 KO mice are manifold. We examined synaptic transmission in autaptic hippocampal neurons from CAPS1 KOs (data not shown) as well as respiratory brainstem function in newborn CAPS1 KOs at the level of hypoglossal nerve activity (data not shown) and found no phenotypic changes. This excludes a general synaptic transmission deficit as the cause of perinatal death of CAPS1 KOs.

Secretion from Heterozygous CAPS1 KO Chromaffin Cells

Because CAPS1 was discovered in PC12 cells and is thought to act as an LDCV-specific regulator of secretion, we analyzed LDCV secretion from KO adrenal chromaffin cells, one of the best-characterized model systems of regulated secretion.

In chromaffin cells, secretory granules can reside in four pools representing different functional states or maturation steps. The size of these pools and the rate of vesicle transition between them can be assayed with high-time resolution patch-clamp capacitance measurements. Granules from the *Depot* pool translocate to the plasma membrane to enter the docked but unprimed granule pool, *UPP*. Granules in the *UPP* are primed into the slowly releasable pool, *SRP*, from where they can enter the rapidly releasable pool, *RRP*. Granules in the *SRP* and *RRP* can fuse with the plasma membrane, but with different rate constants (~3–6 s^{-1} versus ~20–50 s^{-1}) (Ashery et al., 2000).

Deletion of one *CAPS1* allele in heterozygous KOs resulted in a significant reduction of CAPS1 expression in the adrenal gland of P30 animals (Figure 1E; see also Figure 1C for corresponding data from brain). Because of this gene dosage effect, we performed electrophysiological recordings on adrenal slices from P30 heterozygous CAPS1 KOs and wt littermates.

Increases in membrane capacitance (C_m) resulting from Ca^{2+}-dependent exocytosis were monitored using whole-cell patch-clamp recordings on single chromaffin cells stimulated either by depolarization or by flash photolysis of caged Ca^{2+}. Stimulation with a voltage protocol consisting of six 10 ms depolarizations
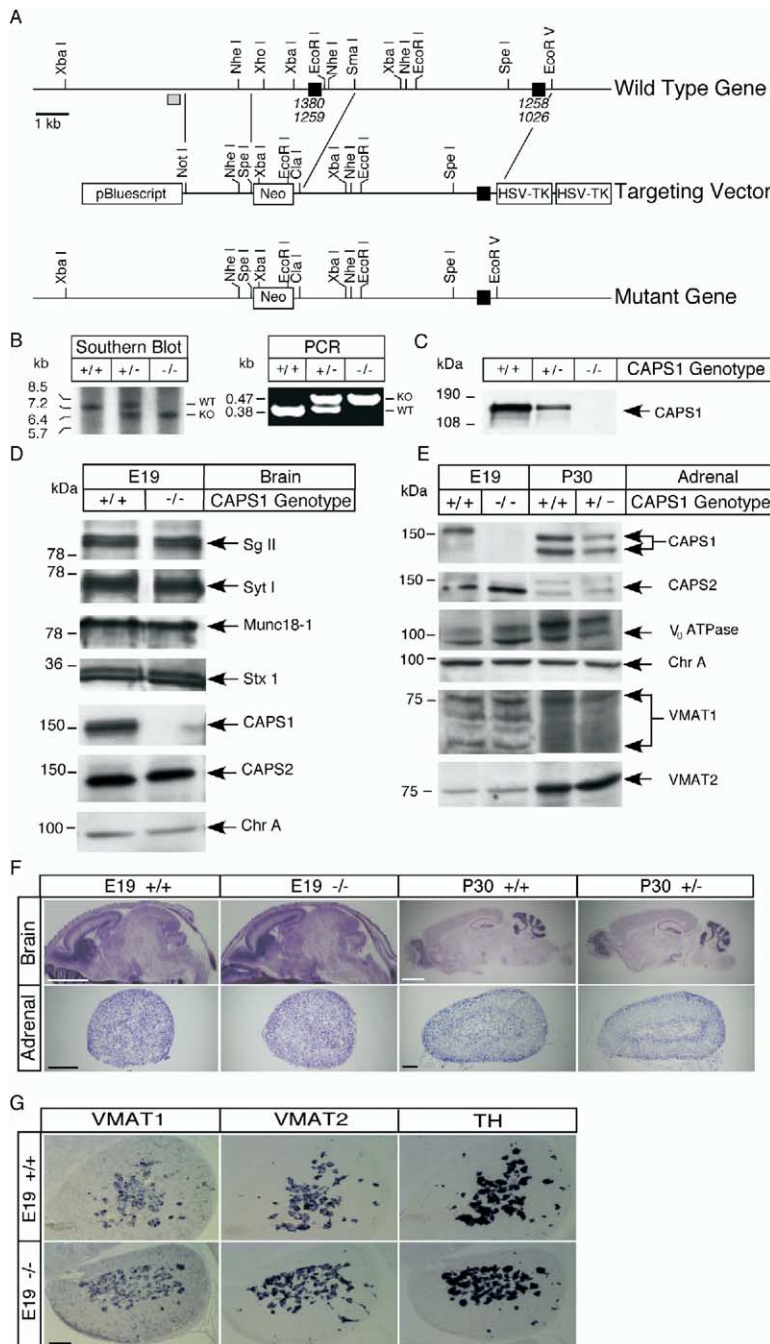
Figure 1. Generation, Protein Expression, and Morphology of CAPS1 KO Mice

(A) Deletion of murine *CAPS1* gene. Maps of the wild-type (wt) *CAPS1* gene, the targeting vector, and the resulting mutant gene are shown. Positions of exons (black boxes with bp of corresponding cDNA) and restriction enzyme sites are indicated. The gray box indicates the position of a probe used to identify the mutant allele. Neo, neomycin resistance gene; HSV-TK, thymidine kinase gene.

(B) Southern blot and PCR analyses. Mouse tail DNA from E19 wt mice (+/+) and mice heterozygous (+/–) or homozygous (–/–) for the mutation in the *CAPS1* gene were analyzed. Positions of bands representing wt and mutant (KO) alleles are indicated.

(C) CAPS1 expression in CAPS1 KO mice. Brain homogenates (20 μg protein per lane) from E19 mice were analyzed by Western blotting using anti-CAPS1 antibodies. Genotypes as in (B).

(D) Expression of presynaptic proteins in brain samples of CAPS1 KO mice. Brain homogenates (20 μg protein per lane) from E19 mice were analyzed by Western blotting using antibodies against the indicated proteins. Genotypes as in (B). Sg II, Secretogranin 2; Syt I, Synaptotagmin 1; Stx 1, Syntaxin 1; Chr A, Chromogranin A.

(E) Expression of vesicular proteins in adrenal glands of CAPS1 KO mice. Adrenal homogenates (25 μg protein per lane) were analyzed by Western blotting using antibodies against the indicated proteins. V_o ATPase, V_o subunit of vesicular H^+-ATPase; Chr A, Chromogranin A; VMAT, vesicular monoamine transporter.

(F) Morphology of brain and adrenals of CAPS1 KO mice. Tissues of E19 and P30 mice were sectioned and processed for cresyl violet staining. Genotypes as in (B). White scale bar, 2 mm; black scale bar, 200 μm.

(G) Distribution of VMATs and tyrosine hydroxylase (TH) expression in adrenals from CAPS1 KO mice. Adrenal glands of E19 mice were sectioned and processed for immunohistochemistry using antibodies against VMAT1, VMAT2, and TH. Genotypes as in (B). VMAT, vesicular monoamine transporter; TH, tyrosine hydroxylase. Scale bar, 50 μm.

followed by four 100 ms depolarizations delivered 300 ms apart (Figure 2A, top) induced voltage-gated Ca^{2+} influx and robust C_m increases in wt cells. The 10 ms depolarizations cause the fusion of the immediately releasable pool, *IRP*, which corresponds to a fraction of the readily releasable granules in the *RRP* that are closely associated with Ca^{2+} channels. The subsequent 100 ms depolarizations elicit the fusion of the remainder of the *RRP* (Voets et al., 1999). The depolarization-evoked C_m increases in heterozygous KO cells were only about 70% of those in wt control cells (Figure 2A, bottom). Statistical analysis showed that both the *IRP*

and *RRP* were significantly reduced in heterozygous CAPS1 KO cells, although the amplitude of voltage-gated Ca^{2+} currents remained unchanged (Figures 2B–2D; Table S1 in the Supplemental Data available with this article online). To investigate possible changes in the Ca^{2+}-dependent kinetics of exocytosis or in granule recruitment, we stimulated wt and heterozygous CAPS1 KO cells using flash photolysis of the photolabile Ca^{2+} cage NP-EGTA. This resulted in stepwise, uniform increases in $[Ca^{2+}]_i$ to 20–30 μM (Figure 2E, top). Again, strikingly different secretory responses were obtained for wt and heterozygous CAPS1 KO cells (Figure 2E,
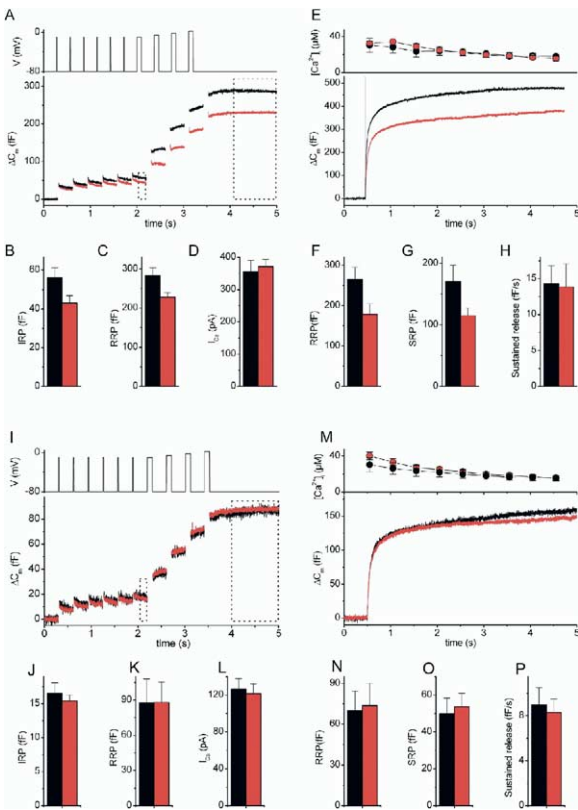
Figure 2. LDCV Secretion in Slices from E19 Homozygous and P30 Heterozygous CAPS1 KO Chromaffin Cells

(A) Voltage protocol (top) and resulting average capacitance increase (ΔC_m) in P30 chromaffin cells from wt (n = 19 cells, four animals) and heterozygous CAPS1 KO (n = 24 cells, four animals) mice. (B) IRP, determined as the average ΔC_m during the time period indicated by the leftmost dashed rectangle in (A). (C) RRP, determined as the average ΔC_m during the time period indicated by the rightmost dashed rectangle in (A). (D) Peak Ca^{2+} current amplitude. (E) Averaged high-time resolution recordings of membrane capacitance in response to flash photolysis of Ca^{2+} bound NP-EGTA from wt (black; n = 18 cells, four animals) and heterozygous CAPS1 KO (red; n = 21 cells, four animals) chromaffin cells. The average intracellular Ca^{2+} concentration following the flash is shown in the upper trace. (F–H) Analysis of the two burst components, RRP and SRP, revealed a similar reduction in amplitude for both pools, while the rate of sustained release was unchanged. (I) Voltage protocol (top) and resulting average capacitance increase (ΔC_m) in E19 chromaffin cells from wt (n = 13 cells, two animals) and homozygous CAPS1 KO (n = 28 cells, three animals) mice. (J) IRP, determined as the average ΔC_m during the time period indicated by the leftmost dashed rectangle in (I). (K) RRP, determined as the average ΔC_m during the time period indicated by the rightmost dashed rectangle in (I). (L) Peak Ca^{2+} current amplitude. (M) Averaged high-time resolution recordings of membrane capacitance in response to flash photolysis of Ca^{2+} bound NP-EGTA from wt (black; n = 16 cells, two animals) and homozygous CAPS1 KO (red; n = 25 cells, three animals) E19 chromaffin cells. The average intracellular Ca^{2+} concentration following the flash is shown in the upper trace. (N–P) Kinetic analysis of the capacitance traces revealed that the two burst components, RRP and SRP, and the rate of sustained release are unchanged. Error bars indicate standard error of the mean.

bottom). For both genotypes, the C_m increase consisted of a fast initial phase, the exocytotic burst, followed by a slower sustained phase of secretion. The exocytotic burst represents exocytosis of all fusion-competent granules, and the sustained component is due to recruitment and subsequent fusion of new granules. The exocytotic burst of individual flash responses can be fitted by the sum of two exponential terms, with the fast and slower component corresponding to the exocytosis of granules from two distinct populations of fusion-competent vesicles, the *SRP* and *RRP* (Ashery et al., 2000; Voets et al., 1999). As predicted on the basis of the depolarization experiments (Figure 2A), *SRP* and *RRP* were significantly reduced to a similar degree in heterozygous CAPS1 KO cells as compared to wt controls (~70% of wt levels; p < 0.02), while sustained release was unchanged (Figures 2F–2H; Table S1). The time constants for fusion of granules from the *SRP* and *RRP* were not different between wt and heterozygous CAPS1 KO cells (data not shown), indicating that the kinetics of Ca^{2+}-triggered fusion are not altered in the partial absence of CAPS1.

These data show that reduction of CAPS1 expression by 35% leads to a concomitant and comparable 30%–35% reduction in releasable granule pools. This pool reduction could be explained if CAPS1 acted as a rate-limiting LDCV priming factor (Hay and Martin, 1992), or if CAPS1 functioned upstream of the priming reaction, i.e., in the biogenesis, stability, trafficking, or docking of LDCVs. Deficits in the latter processes would ultimately lead to a decrease in releasable granule pools.

Secretion from Homozygous
CAPS1 KO Chromaffin Cells
We next performed electrophysiological recordings in adrenal slices from littermate wt and homozygous CAPS1 KO E19 embryos. Astonishingly, using the same depolarization and flash photolysis protocols applied to heterozygous chromaffin cells (Figures 2A–2H), we found no changes in secretion between homozygous KO and wt control cells as determined by capacitance measurements. Statistical analysis revealed no significant differences between wt and homozygous CAPS1 KO cells in either the size of *IRP* and *RRP* or the amplitude of voltage-gated Ca^{2+} currents (Figures 2I–2L; Table S1). When we stimulated wt and homozygous CAPS1 KO cells using flash photolysis of the photolabile Ca^{2+} cage NP-EGTA, which resulted in stepwise, uniform increases in $[Ca^{2+}]_i$ to 20–40 μM (Figure 2M, top), we again measured very similar secretory responses in wt and homozygous CAPS1 KO cells (Figure 2M, bottom). Very similar values were obtained for the size of the *SRP* and *RRP* and for the rate of sustained secretion (Figures 2N–2P; Table S1). Moreover, the time constants for fusion of the *SRP* and *RRP* were not significantly different between wt and homozygous CAPS1 KO cells (data not shown), indicating that vesicle fusion kinetics are not altered in the absence of CAPS1 on E19.

Expression of CAPS Isoforms in Murine
Adrenal Gland
Two possible mechanisms may account for the finding that chromaffin granule secretion from P30 heterozy-
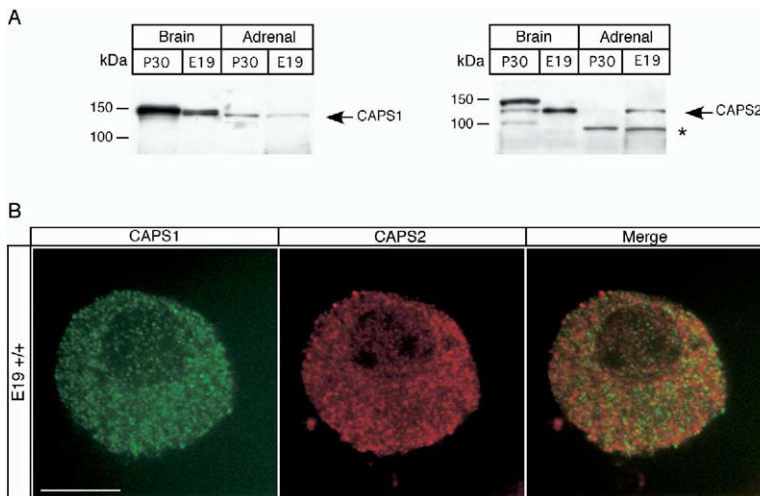
Figure 3. Expression Levels of CAPS1 and CAPS2 Isoforms in Adrenal Glands during Development

Expression of CAPS1 and CAPS2 proteins in mouse adrenal and brain. (A) Homogenates from brains and adrenals (18 μg protein per lane) from P30 and E19 mice were analyzed by SDS-PAGE and immunoblotting using antibodies against CAPS1 and CAPS2. Asterisk indicates an unspecific band detected by CAPS2 antibodies. (B) Confocal images through an embryonic (E19) chromaffin cell immunolabeled with anti-CAPS1 (green, left) and anti-CAPS2 (red, middle) antibodies. Overlay of both channels (right) revealed almost no colocalization between both isoforms. Note that different antibodies than in (A) were used (see Experimental Procedures). Scale bar, 5 μm.

gous CAPS1 KO chromaffin cells—where CAPS1 expression is at about 60%–70% of wt levels—is reduced by about 30%, while E19 homozygous KO cells lacking CAPS1 are not affected (Figure 2). Either embryonic chromaffin cells utilize a vesicle maturation pathway that does not depend on CAPS proteins (e.g., involving Munc13 isoforms), or CAPS2 compensates for the CAPS1 loss in embryonic but not in adult cells.

CAPS1 and CAPS2 expression levels in brain are differentially regulated during development (Speidel et al., 2003). CAPS1 protein expression is similar to that of synaptic markers. It is first detectable late in embryogenesis (E14) and increases to reach a plateau 20 days after birth, when most synapses have been formed. In contrast, CAPS2 protein expression levels are more stable during development and even higher in the embryonic brain than in later phases of development. To test whether CAPS1 and CAPS2 expression in the adrenal gland is also differentially regulated during development, we examined corresponding mRNA and protein levels by in situ hybridization, immunocytochemistry, and Western blot analysis of brains and adrenal glands from P30 and E19 mice.

In situ hybridization experiments with isoform-specific radiolabeled antisense oligonucleotides (Speidel et al., 2003) showed that CAPS1 mRNA is abundantly and specifically expressed in cells of the P30 mouse adrenal medulla. CAPS1 mRNA levels in E19 and P30 mouse chromaffin cells were similar (Figure S1A). No CAPS1 mRNA was detectable in adrenal sections obtained from homozygous CAPS1 KOs (data not shown). In contrast, when CAPS2-specific antisense oligonucleotides were used, corresponding mRNA levels were found to be high only in E19 mouse chromaffin cells, but at or below the detection limit in adult mouse adrenal gland (Figure S1A).

Immunocytochemical experiments showed that the differential developmental regulation of CAPS1 and CAPS2 mRNA expression levels is reflected by the corresponding protein expression levels. Using CAPS1 and CAPS2 isoform-specific antibodies, we immunodetected CAPS1 and CAPS2 in chromaffin cells of the E19 mouse adrenal gland medulla. However, in chromaffin cells of P30 mouse adrenal glands, only CAPS1 but not CAPS2 was detectable (Figure S1B). Western blot analyses of brain and adrenal homogenates from E19 and P30 mice showed that CAPS1 expression is stable or upregulated during development, while CAPS2 expression is downregulated (Figure 3A). This effect was most striking in the adrenal, where CAPS1 is barely detectable at E19 and robustly expressed in P30 animals, while CAPS2 is present only in E19 tissue but absent at P30 (Figure 3A). After determining the titers of our anti-CAPS antibodies (see Experimental Procedures), we estimated the relative amounts of CAPS1 and CAPS2 in the different tissues at different developmental stages by densitometric analyses of Western blots. CAPS1 protein levels in the adult adrenal gland were at least two times higher than corresponding CAPS2 levels. In contrast, CAPS2 protein levels in adrenals from E19 mice were about eight times higher than corresponding CAPS1 levels (Figure 3A). The situation in brain tissue is similar but less pronounced, and both full-length CAPS2 and a smaller splice variant of CAPS2, most likely lacking a 333 bp exon (Speidel et al., 2003), are expressed in adult mouse brain (Figure 3A).

To investigate the subcellular localization of CAPS1 and CAPS2, we performed immunocytochemical analyses on isolated chromaffin cells from E19 adrenal glands. Most CAPS1 and CAPS2 immunoreactivity was localized to small punctate structures (Figure 3B). Interestingly, very little overlap between CAPS1 and CAPS2 immunoreactive structures was observed (Figure 3B), indicating that the two CAPS isoforms may reside on different populations of LDCVs.

Thus, CAPS1 and CAPS2 levels are inversely correlated, and the two isoforms are most likely targeted to different subpopulations of LDCVs in mouse chromaffin cells, and the fact that loss of one *CAPS1* allele leads to reduced secretory activity in P30 chromaffin cells, as determined by C_m measurements, while complete loss of CAPS1 expression in E19 mice has no effect (Figure 2), can in part be explained by redundant expression of CAPS2 only in embryonic but not in adult adrenal tissue.
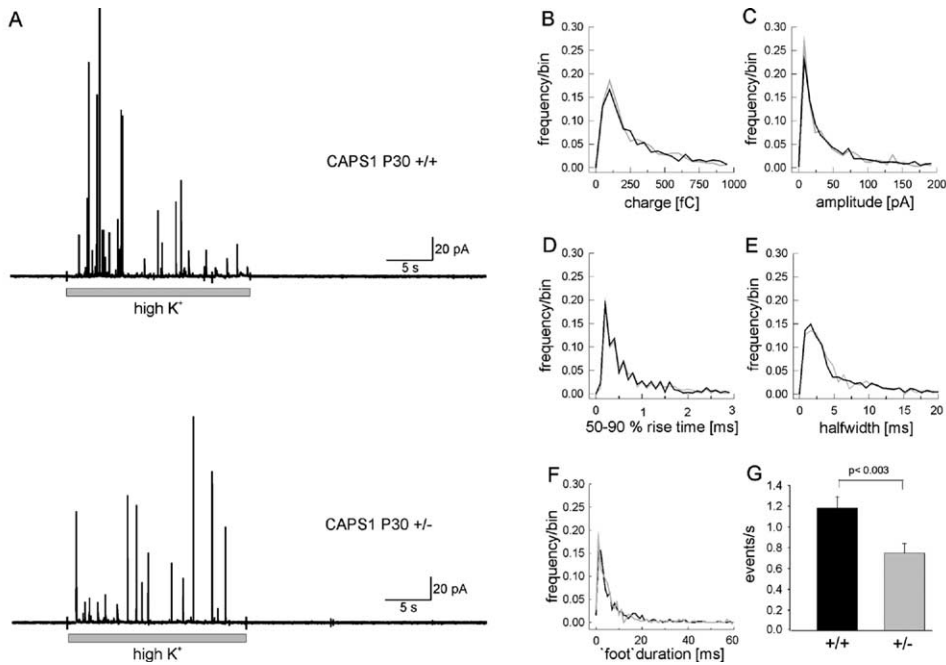
Figure 4. Frequency of Amperometric Events in P30 Heterozygous CAPS1 KO Mice

(A) Representative traces of carbon fiber amperometry measurements from isolated chromaffin cells of P30 wt and heterozygous CAPS1 KO mice. Secretion was triggered by extracellular application of 80 mM K$^+$ as indicated (gray bar).

(B–G) Frequency distribution of individual single spike parameters obtained from the analysis of 21 wt and 21 heterozygous CAPS1 KO cells. Charge (B), amplitude (C), 50%–90% rise time (D), half-width (E), and foot duration (F) were indistinguishable between both groups, while the frequency of amperometric events in heterozygous CAPS1 KO cells was significantly reduced by approximately 35% compared to wt cells ([G]; p < 0.003). Error bars indicate standard error of the mean.

Single Secretory Granule Fusion Events in P30 Heterozygous CAPS1 KO Chromaffin Cells

We next performed amperometric measurements, which detect the catecholamines released from chromaffin granules by oxidation on the surface of a carbon fiber electrode (Bruns and Jahn, 1995).

Typically, the ratio between quantal monoamine content and vesicle volume is rather constant (Bruns et al., 2000). The observed reduction in secretion from P30 heterozygous CAPS1 KO mice (Figure 2) could be due either to a reduced number of vesicles residing in RRP and SRP or to a reduced size of individual vesicles. To distinguish between these possibilities, we stimulated isolated chromaffin cells with 80 mM KCl for 20 s and measured the resulting amperometric spikes during the KCl application with a 5 μm carbon fiber electrode. The spike frequency in heterozygous CAPS1 KO cells was reduced to ~65% of wt levels (1.18 ± 0.11 events/s [n = 21] in control cells and 0.75 ± 0.09 events/s [n = 21] in heterozygous CAPS1 KO cells; p ≤ 0.003; Figures 4A and 4G; Table S2). This reduction is in agreement with the observed reduction in CAPS1 expression levels (Figures 1C and 1E) and secretion measured in capacitance recordings (Figure 2). No difference in charge, amplitude, 50%–90% rise time, half-width, and foot duration of spikes was observed (Figures 4B–4F).

Thus, the reduction in secretion from chromaffin cells of P30 heterozygous CAPS1 KO mice observed in capacitance measurements following depolarization or flash photolysis (Figure 2) can be attributed to a reduc-

tion in the number of releasable vesicles in the RRP and SRP.

Single Secretory Granule Fusion Events in E19 Homozygous CAPS1 KO Chromaffin Cells

We next performed amperometric recordings on isolated E19 chromaffin cells of homozygous CAPS1 KO mice. Based on our capacitance recordings (Figure 2), we expected to see no difference in frequency and single spike parameters between wt and CAPS1 KO cells. Surprisingly, measurements from four different animals revealed that the frequency of amperometric spikes in CAPS1 KO cells was only ~40% of wt levels (1.85 ± 0.13 events/s [n = 27] in control cells and 0.73 ± 0.22 events/s [n = 26] in homozygous CAPS1 KO cells; p ≤ 0.0001; Figures 5A and 5G; Table S2). Like in heterozygous animals, the single spike characteristics were unchanged (Figures 5B–5F; Table S2).

To test the specificity of this finding, we performed rescue experiments by overexpressing a CAPS1-GFP fusion protein in E19 CAPS1 KO cells. Reintroduction of CAPS1-GFP into CAPS1 KO chromaffin cells led to a complete recovery of the frequency of amperometric spikes (2.05 ± 0.52 events/s [n = 9]; Figure 5G), while the introduction of GFP alone had no effect (data not shown). Thus, the reduction of spike frequency mediated by the selective loss of CAPS1 expression is specific and reversible.

The discrepancy between capacitance and amperometry recordings in E19 homozygous CAPS1 KO mice
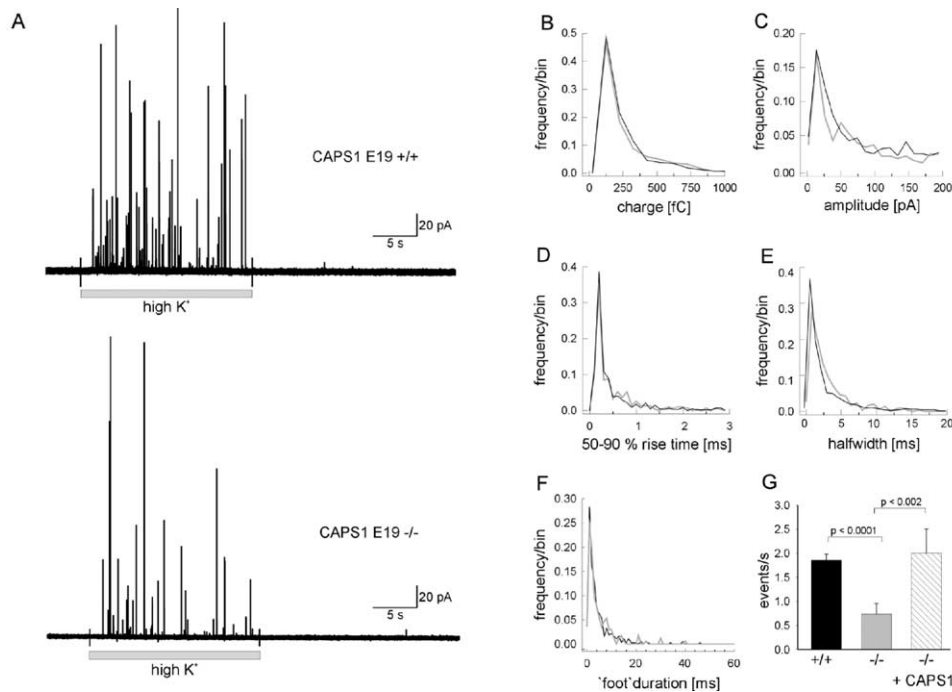
Figure 5. Frequency of Amperometric Events in E19 Homozygous CAPS1 KO Mice

(A) Representative traces of carbon fiber amperometry measurements from isolated chromaffin cells of E19 wt and homozygous CAPS1 KO mice. Secretion was triggered by extracellular application of 80 mM K$^+$ as indicated (gray bar).

(B–G) Frequency distribution of individual single spike parameters obtained from the analysis of 21 wt and 21 homozygous CAPS1 KO cells. Charge (B), amplitude (C), 50%–90% rise time (D), half-width (E), and foot duration (F) were indistinguishable between both groups, while the frequency of amperometric events in homozygous CAPS1 KO cells was significantly reduced by approximately 60% compared to wt cells ([G]; p < 0.0001). Reintroduction of CAPS1 into CAPS1 KO cells led to a complete recovery of the frequency of amperometric events ([G]; p < 0.002). Error bars indicate standard error of the mean.

(Figures 2 and 5) prompted us to perform simultaneous capacitance and amperometry recordings following flash photolysis of NP-EGTA. Measurements from 12 control and 12 CAPS1 KO cells confirmed that the capacitance response was identical and the amperometric response was reduced in CAPS1 KO cells as compared to wt control cells (Figure S2).
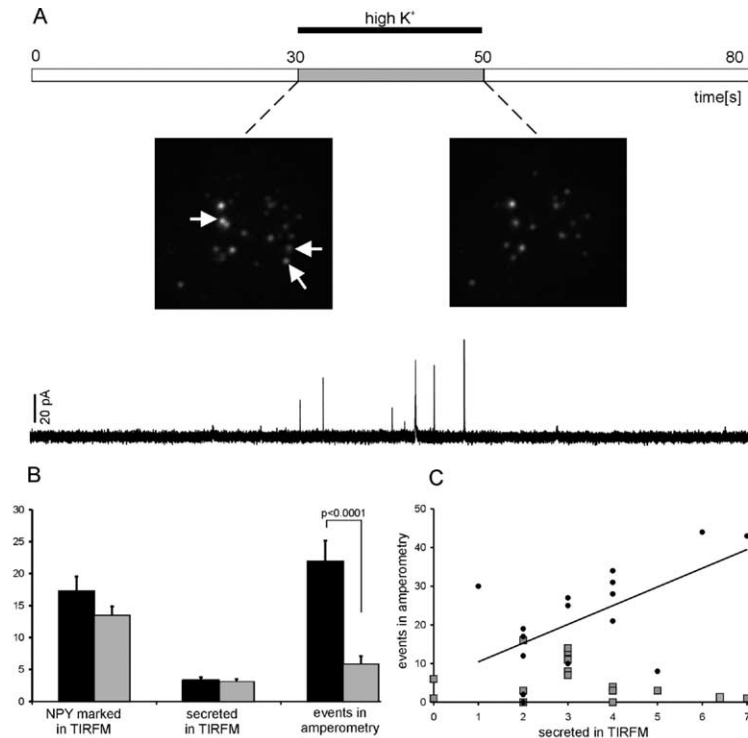
Two alternative scenarios might account for this phenomenon. First, CAPS1 might have a role in both exo- and endocytosis. The absence of CAPS1 would lead to the fusion of fewer vesicles, as evidenced by the lower spike frequency (Figures 5A and 5G), but concomitantly to a decrease of endocytosis by exactly the same magnitude. In view of our knowledge about CAPS function, this possibility is highly unlikely. Second, CAPS1 might be involved in the filling of vesicles with catecholamines. The absence of CAPS1 would lead to the generation of empty vesicles, which in the embryonic state would still be correctly docked and primed at the plasma membrane. Fusion of these vesicles upon stimulation would then lead to an increase in capacitance of the plasma membrane but would not be detected in amperometric recordings. The existence of such empty vesicles in chromaffin cells has been demonstrated previously (Gong et al., 2003; Tabares et al., 2001).

To support our electrophysiological findings on E19 CAPS1 KO chromaffin cells with an independent technique, we performed total internal reflection fluorescence microscopy (TIRFM) on E19 CAPS1 KO cells and their wt counterparts. The TIRFM technology allows to visualize single vesicles arriving at the plasma membrane, where they lose their mobility following docking and priming. Additionally, the fusion of vesicles following depolarization can be investigated reliably (Becherer et al., 2003; Steyer et al., 1997).

To specifically label LDCVs, we infected isolated chromaffin cells from E19 wt and CAPS1 KO mice with a virus expressing Neuropeptide Y (NPY) fused to Venus, a yellow variant of GFP. After a resting period of 30 s, during which we counted the number of labeled vesicles at the plasma membrane (Figures 6A and 6B), secretion was triggered by extracellular application of 80 mM K$^+$ for 20 s. During this application, a fraction of membrane-associated vesicles fused with the plasma membrane as detected by a sudden loss of fluorescence in TIRFM. Simultaneously, we measured catecholamine secretion by amperometry (Figures 6A and 6B). Quantitative analysis of the data from 16 wt (two animals) and 16 CAPS1 KO cells (two animals) revealed that the number of fused vesicles measured by TIRFM was identical between the two groups. In contrast, the number of fusion events measured in amperometry was again significantly lower (~30% of wt levels; p < 0.0001) in CAPS1 KO cells (Figure 6B). Plotting the fusion events in amperometry against the fusion events in TIRFM revealed a linear correlation for wt cells but no correlation for CAPS1 KO cells (Figure 6C).

The combined TIRFM/amperometry measurements

Figure 6. Fusion in E19 CAPS1 KO Cells Measured by Simultaneous Amperometry and TIRFM

(A) Example of a homozygous CAPS1 KO E19 cell measured simultaneously with TIRFM and carbon fiber amperometry. Vesicles were labeled by overexpression of a NPY-Venus construct, and secretion was triggered by application of 80 mM K$^+$ as indicated in the stimulus protocol (upper panel). TIRFM images of NPY-Venus-labeled vesicles before (left) and after (right) stimulation are shown in the middle panel. Vesicles that fused during stimulation are marked with arrows in the left image. The corresponding trace of the amperometric measurement during stimulation is shown in the lower panel.

(B) Quantitative comparison of averaged wt (n = 16 cells, two animals; white bars) and CAPS1 KO (n = 16 cells, two animals; gray bars) cells measured simultaneously with TIRFM and amperometry. The left pair of columns shows the number of vesicles marked with NPY-Venus at the beginning of the experiment. No significant difference in vesicle number could be observed between the two populations. During stimulation, the number of secreted vesicles as visualized by TIRFM was also not significantly changed (middle pair of columns). The right pair of columns shows the number of amperometric events recorded simultaneously during high-K$^+$ application. The number of events in CAPS1 KO cells was significantly reduced to approximately 30% of wt levels (p < 0.0001). Error bars indicate standard error of the mean.

(C) Plot of exocytotic events measured by TIRFM versus exocytotic events measured simultaneously by amperometry. As expected, there is a linear correlation between both secretion assays in wt cells (black circles), but no correlation in CAPS1 KO cells (gray squares).

are in excellent agreement with the data obtained from single capacitance, single amperometry, and combined capacitance/amperometry measurements. The data indicate that the absence of CAPS1 in chromaffin cells leads to a defect in the biogenesis, stability, catecholamine filling, or catecholamine storage of a subset of LDCVs, while the capability of LDCVs to fuse with the plasma membrane in a Ca^{2+}-dependent manner remains unaffected.

Ultrastructure of Homozygous and Heterozygous CAPS1 KO Chromaffin Cells

We next analyzed the ultrastructure of mutant chromaffin cells to examine possible deficits in secretory granule biogenesis or granule docking at the plasma membrane, which should be detectable as a reduction in the overall number of granules and in the number of docked vesicles, respectively.

Ultrathin sections from P30 and E19 adrenals were analyzed electron microscopically (Figures 7A and 7B). Signs for a degeneration of vesicles or of other cellular organelles, or signs of apoptosis, were not detectable in either P30 heterozygous or E19 KO chromaffin cells, and no accumulation of vesicular structures lacking the typical dense core was detected in E19 chromaffin cells. To investigate whether LDCV numbers in CAPS1 mutants at one of the studied developmental stages are changed, we examined the number and distribution of LDCVs in wt and CAPS1 mutant cells. In E19 homozygous KO chromaffin cells (n = 19 cells, two animals), vesicle numbers and distribution were indistinguishable

from wt values (n = 21, two animals; Figure 7D). However, in P30 chromaffin cells from heterozygous CAPS1 KO cells, we found a reduction in the number of LDCVs within a distance of up to 200 nm from the plasma membrane (i.e., morphologically docked vesicles; 71% ± 6% of wt; p < 0.026; Figure 7C). Numbers of LDCVs more distant from the plasma membrane were not altered (Figure 7C).

Thus, the observed reduction in secretion in P30 heterozygous CAPS1 KO cells is due to a reduction in the number of membrane-proximal LDCVs. For homozygous E19 KO cells, the normal number of LDCVs excludes an effect of CAPS1 loss on secretory granule biogenesis or granule docking.

Determination of Catecholamine and Catechol Levels in Intact Adrenals

To investigate whether the reduced frequency of amperometric signals in CAPS1 KO chromaffin cells is reflected by a reduction of total catecholamine levels, we determined the monoamine content in homogenates of adrenal glands by HPLC. Only dopamine (DA) levels were significantly decreased in adrenals from homozygous KO mice (n = 12 animals) to about 71% ± 4% of wt levels (n = 12 animals; p < 0.02), whereas adrenaline (ADR) and NA levels were not altered (Figure 8A). As DA usually represents only a minor fraction of the total catecholamine pool in chromaffin cells (2%–10%), the observed overall change in KO cells was surprisingly low given the robust difference in our amperometric records.
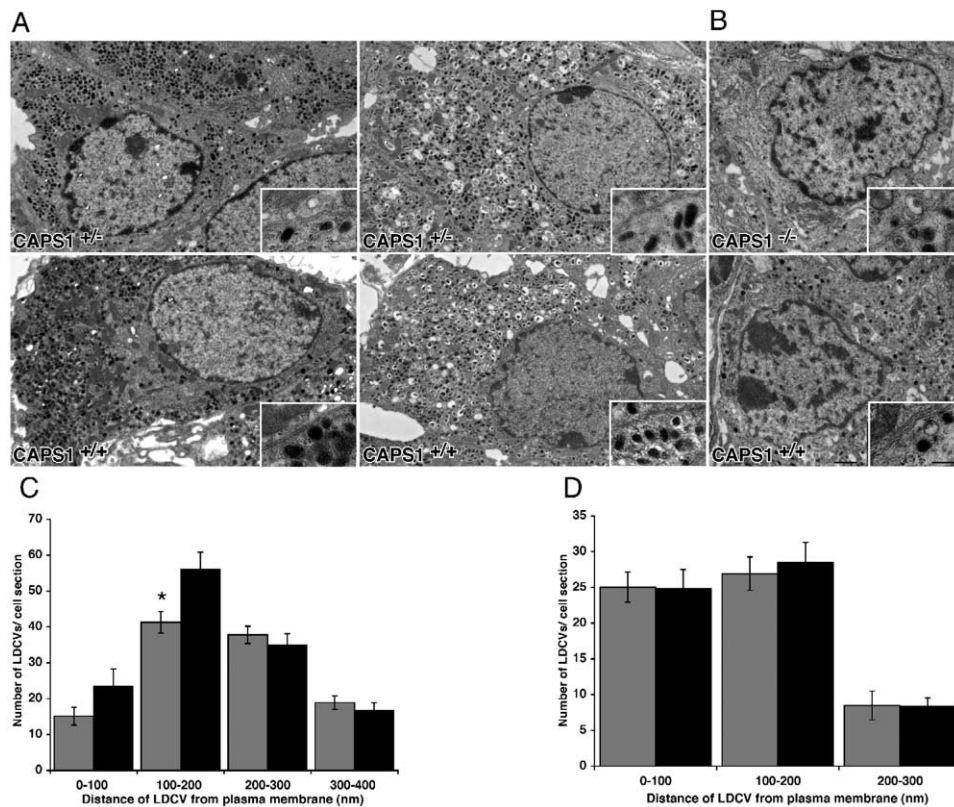
Figure 7. Ultrastructure of Chromaffin Cells from Heterozygous and Homozygous CAPS1 KO Mice

(A and B) Representative electron micrographs of chromaffin cells from P30 (A) and E19 (B) CAPS1 wt (+/+), heterozygous (+/−), and homozygous (−/−) KO mice. Scale bars, 1 μm and 200 nm (inset). (C) Quantitative analysis of LDCVs of 21 wt and 19 heterozygous CAPS1 KO chromaffin cells from P30 mice (two animals for each genotype). The fraction of "morphologically docked" vesicles (<200 nm from the plasma membrane) is reduced in CAPS1 heterozygous animals. *p < 0.05. (D) Quantitative analysis of LDCVs of chromaffin cells from E19 wt (n = 16 cells, two animals) and CAPS1 KO (n = 16 cells, two animals) mice. The overall number and distribution of vesicles is similar. Error bars indicate standard error of the mean.

Inhibition of catecholamine uptake into chromaffin granules by reserpine causes a massive increase of cytosolic catechols, which results from the rapid degradation of catecholamines accumulating in the cytosol (Mosharov et al., 2003). As all our physiological data indicated a defect in catecholamine uptake and/or storage in CAPS1 KO chromaffin granules (Figures 5 and 6), we expected a similar catechol accumulation in CAPS1 KO chromaffin cells. Indeed, we found the levels of the NA/ADR metabolite 3,4-dihyroxyphenylethyleneglycol (DOPEG) in CAPS1 KO adrenals to be strongly increased to 345% ± 60% of wt levels (twelve animals; p < 0.0012). In contrast, the levels of the DA metabolite 3,4-dihydroxyphenylacetic acid (DOPAC), which in wt adrenals are ten times lower than DOPEG levels, and of the DOPEG methylation product 3-methoxy-4-hyroxyphenylethyleneglycol (MOPEG), which are usually similar to the DOPEG levels under wt conditions, were only slightly increased over the corresponding wt levels (Figure 8B).

As an alternative approach to estimate total monoamine content, we treated adrenal gland sections from E19 wt and CAPS1 KO cells with glyoxylic acid, which reacts with monoamines, leading to fluorescence signals. Fluorescence intensity was diffuse and lower in

chromaffin cells from homozygous CAPS1 KOs as compared to control tissue (Figure 8C). As catecholamines are 10,000 times more concentrated in vesicles than in the cytosol (Parsons, 2000), the largest fraction of the respective fluorescence signals is most likely derived from vesicular catecholamine pools, whereas cytosolic catecholamine levels are probably at or below the detection limit of this assay. This is reflected by the preferentially punctate signals in control cells as compared to the more diffuse fluorescence observed in CAPS1 KO cells (Figure 8C, insets).

These data show that, except for DA, overall catecholamine levels are well maintained in CAPS1 KO chromaffin cells. However, cytosolic catechol levels in CAPS1 KO chromaffin cells are strongly increased, indicating that a significant proportion of catecholamines is shifted from vesicular to cytosolic pools and degraded.

Discussion

We show here that CAPS1, a regulator of LDCV secretion, is essential for postnatal survival but not for embryonic development. In physiological experiments, we made the unexpected observation that, in the absence of CAPS1, embryonic chromaffin cells release up to
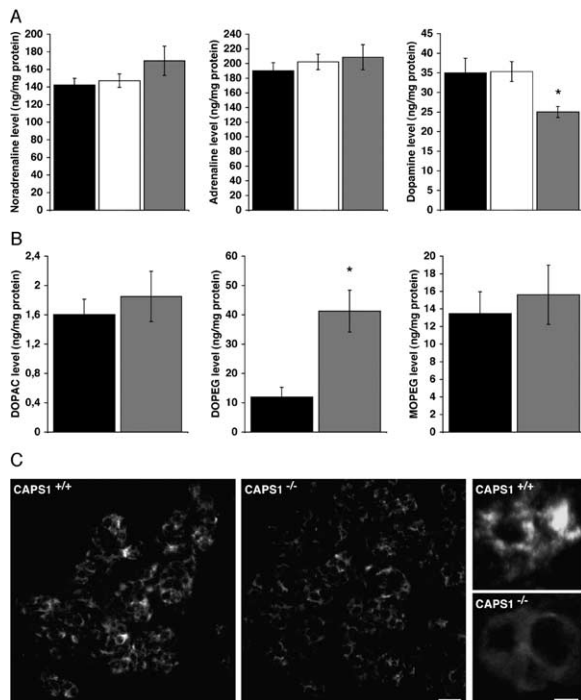
Figure 8. Tissue Catecholamine Content in Adrenals from CAPS1 KO Mice

(A) HPLC analysis of total adrenal content of catecholamines. Adrenal homogenates of 12 CAPS1 wt (+/+), 21 CAPS1 (+/−), and 12 CAPS1 (−/−) E19 KO mice were used for HPLC assessment. Results are presented as the mean ± SEM. Only DA levels are significantly decreased (71% ± 4%; p < 0.02) compared to wt (100%). NA and ADR levels are not significantly altered (p = 0.13 [NA] and p = 0.37 [ADR]) in CAPS1 KO mice compared to wt mice.

(B) HPLC analysis of total catechol content of adrenals. Adrenal homogenates of 12 CAPS1 wt (+/+) and 12 CAPS1 (−/−) E19 KO mice were used for HPLC assessment. Results are presented as the mean ± SEM. DOPEG levels are significantly increased (345% ± 60%; p < 0.0012) compared to wt (100%). DOPAC and MOPEG levels are only slightly increased over wt levels (p = 0.53 [DOPAC] and p = 0.61 [MOPEG] in CAPS1 KO mice compared to wt mice).

(C) Glyoxylic acid-induced catecholamine fluorescence in adrenal glands from E19 wt and CAPS1 KO mice. Sections from unfixed adrenal glands were stained simultaneously, and pictures were captured with a confocal laser scanning microscope using identical settings for KO and wt samples. Note the reduced fluorescence intensity in adrenal medulla from CAPS1 KO compared to wt mice. Scale bars, 20 μm and 5 μm (enlarged images).

70% empty LDCVs lacking catecholamine content (Figures 5 and 6). This phenotype is paralleled by a 25%–30% reduction in total adrenal DA levels (Figure 8A), a 3.5-fold increase of the cytosolic metabolite DOPEG (Figure 8B), and a decrease in vesicular catecholamines as assessed by glyoxylic acid cytochemistry (Figure 8C), but normal ultrastructure and LDCV density (Figure 7D), and normal expression of transmitter carriers and selected transmitter biosynthetic enzymes (Figures 1E and 1G). In adult heterozygous chromaffin cells lacking one *CAPS1* allele, only secretion of transmitter-filled LDCVs and no release of empty vesicles is observed, but overall secretion is reduced by 30%–35% (Figures

2 and 4) due to an underlying decrease in the number of membrane-proximal LDCVs (Figure 7C).

In homozygous CAPS1 KO chromaffin cells, we observed that up to 70% of all LDCV secretory events that are detectable by capacitance measurements and TIRFM can not be detected by amperometric recording of released catecholamine (Figures 2, 5, and 6 and Figure S2). The only plausible explanation for this finding is that CAPS1 KO cells fuse LDCVs that do not contain catecholamines. The phenomenon that chromaffin cells contain LDCVs that fuse with the plasma membrane without containing catecholamines has been demonstrated previously by patch amperometry (Gong et al., 2003; Tabares et al., 2001). These studies revealed that 7%–8% of chromaffin granules are devoid of catecholamines, and this number increased to 47% of total fusogenic vesicles upon specific blockade of the vesicular monoamine transporter VMAT with reserpine (Tabares et al., 2001). In light of these data, our experimental results on CAPS1 KO cells indicate a role for CAPS1 in catecholamine uptake or storage.

Monoamine uptake into chromaffin granules is mediated by two transporters, VMAT1 and VMAT2, which are driven by a H$^+$ electrochemical gradient generated by a V$_o$ H$^+$ ATPase (Erickson et al., 1996; Parsons, 2000; Schuldiner, 1994). In chromaffin cells, NA synthesis depends on the uptake of its precursor DA into chromaffin granules and its subsequent conversion by intragranular DA-β-hydroxylase (Markoglou and Wainer, 2001). Generation of ADR occurs after leakage of NA from granules and conversion by phenylethanolamine-N-methyltransferase (Henry et al., 1998). Adult differentiated chromaffin cells store either ADR or NA in secretory granules, and cytosolic catecholamines are degraded rapidly. In contrast, embryonic chromaffin cells produce and store all catecholamine types, and cytosolic concentrations are significant, possibly due to less degradation (Iwasa et al., 1999; Mosharov et al., 2003; Peaston and Weinkove, 2004). In both developmental stages, uptake and leakage of catecholamines from granules has to be tightly controlled in order to maintain synthesis of ADR and to guarantee proper granule filling. However, the mechanism of leakage and its control are unknown (Parsons, 2000; Schonn et al., 2003). In neurons, blockade of catecholamine uptake into vesicles due to a VMAT2 KO mutation leads to a dramatic decrease in the total brain levels of all catecholamines, while heterozygous KOs show only minor changes (Wang et al., 1997). In addition, inhibition of monoamine uptake into chromaffin granules by reserpine causes a massive increase of cytosolic catechols, which results from the rapid degradation of catecholamines in the cytosol (Mosharov et al., 2003).

Our finding that DA levels in CAPS1 KO embryonic adrenals are reduced by 25%–30%, while ADR and NA concentrations are normal (Figure 8A), and that the levels of the main NA/ADR metabolite DOPEG are increased dramatically (Figure 8B) is compatible with the notion that these KO chromaffin cells have a selective deficit in granular catecholamine uptake or storage and therefore contain and fuse a significant population of empty granules. In that respect, the CAPS1 KO scenario with about 60%–70% empty vesicles (Figures 5 and 6) is comparable to the heterozygous VMAT2 KO

situation, where in contrast to the homozygous KO, uptake is still operational at reduced rates, and only slight reductions in catecholamine levels are observed in brain (Wang et al., 1997), or to conditions of reserpine-mediated inhibition of monoamine uptake, where catechols were shown to accumulate in the cytosol (Mosharov et al., 2003). Under CAPS1 KO conditions, the shuttling of catecholamines through a subpopulation of vesicles would still be maintained and sufficient to generate normal amounts of NA and ADR, while uptake or storage in a second subpopulation of granules is disturbed, leading to less catecholamine accumulation and breakdown of the cytosolic pools to catechol metabolites. Why DA levels are affected so selectively remains unclear but may be a feature of embryonic chromaffin cells. It is possible that newborn chromaffin cells respond to the CAPS1 loss and the concomitant defect in the uptake or storage of catecholamines in a compensatory manner by increasing synthesis rates and thereby roughly maintain cellular catecholamine levels.

The data obtained with glyoxylic acid cytochemistry (Figure 8C) indicate that individual chromaffin cells have reduced granular catecholamine levels. The intense punctate glyoxylic acid staining seen in wt cells, which most likely resembles catecholamines stored in granula, is less apparent in CAPS1 KO cells. Together with our data on total catecholamine and catechol levels in adrenals, this indicates that catecholamines are either not taken up or not stored in CAPS1 KO granules and therefore diluted into the cytosol and degraded.

Surprisingly, adult heterozygous CAPS1 KO chromaffin cells show no discrepancy between fusion and transmitter release events (Figure 2), indicating an absence of empty granules lacking catecholamine. However, these cells exhibit concordant 25%–30% reductions in secretion and membrane-proximal granule numbers, which is best explained by a selective loss of granules. We postulate a quality control mechanism, according to which, during maturation of the adrenal gland, heterozygous CAPS1 KO chromaffin cells eliminate the empty vesicle population that is initially generated due to the partial lack of CAPS1 and the segregation of CAPS2 to a different granule population (see below).

While all our functional data point to a role of CAPS1 in chromaffin granule transmitter loading or storage, the molecular basis of this effect is unclear. CAPS1 does not interfere with the expression or localization of the proteins essential for uptake activity, i.e., VMATs and the V_o ATPase, as protein levels of VMATs and subunits of the V_o ATPase are not altered in CAPS1 KO chromaffin cells (Figures 1E and 1G), and VMAT distribution to structures resembling secretory granules is normal (data not shown). Nevertheless, CAPS1 could directly affect the function of VMATs or the V_o ATPase and thereby regulate catecholamine uptake or storage. Such a regulatory effect has been described for certain heterotrimeric G proteins (Ahnert-Hilger et al., 2003). $G_\alpha o2$, $G_\alpha q11$, $G_\beta 2$, and $G_\beta 5$ subunits are present on chromaffin granules of the rat adrenal medulla and colocalized with either VMAT1 or VMAT2 (Pahner et al., 2002). Low concentrations of $G_\alpha o2$ inhibit catecholamine accumulation in chromaffin granules to about the

same extent as the general G protein activator GMppNp, while GDPβS has no effect (Pahner et al., 2002), indicating that active heterotrimeric G proteins downregulate the catecholamine content of chromaffin granules by inhibiting catecholamine uptake or storage. Recent studies in *C. elegans* showed that loss-of-function mutations in the heterotrimeric Go protein suppressed the phenotype of *unc-31* (CAPS) mutants (E. Jorgensen, personal communication). This indicates that CAPS acts in the same pathway as heterotrimeric G proteins, exerting its function either by inhibiting vesicular G proteins or by activating, in antagonism to G proteins, VMATs. Alternatively, CAPS may influence granular membrane composition or stability and thereby regulate catecholamine uptake or prevent leakage. The fact that the level of the major ADR/NA metabolite DOPEG is selectively increased while the levels of the main DA metabolite DOPAC are only marginally altered in CAPS1 KOs indicates that, in CAPS1 KO chromaffin cells, DA is still taken up into granules and converted to NA, but NA and ADR leak out of these granules, resulting in their more rapid conversion to DOPEG.

At first glance, the mouse CAPS1 KO phenotype is different from that observed in *Drosophila*, where a 50% decrease in glutamatergic transmission at neuromuscular junctions and a concomitant accumulation of SVs and in particular LDCVs was observed (Renden et al., 2001). The *Drosophila* phenotype was interpreted as an indirect effect of an upstream dysregulation in hormone signaling (Renden et al., 2001), but it is possible that an analysis of direct effects of CAPS loss, e.g., on catecholamine release in mutant flies, will yield data that are compatible with our findings. Whether the functional consequences of CAPS1 action observed in PC12 cells (Ann et al., 1997; Hay and Martin, 1992; Walent et al., 1992) are compatible with a role of CAPS in catecholamine uptake or storage remains to be explored.

Despite the detailed biochemical characterization of CAPS1 interactions with LDCVs, lipids, and plasma membrane proteins or protein components of the fusion machinery (Wassenberg and Martin, 2002), information regarding the physiological function of CAPS proteins, beyond the notion of a general role in controlling LDCV secretion, is scarce. Elhamdani et al. (1999) loaded affinity-purified anti-CAPS1 antibodies into calf chromaffin cells and measured the kinetics of catecholamine release by amperometry and capacitance recordings. They observed a reduction in the frequency of amperometric events by about 80%, which is in agreement with our data (Figures 5 and 6). In addition, a dramatic effect of anti-CAPS1 antibodies on the time course of secretion of individual vesicles was reported (prolonged mean rise time and half-width of amperometric peaks), and a role of CAPS1 in the final stage of Ca^{2+}-triggered secretion at the level of the fusion step was concluded. We measured 614 and 305 individual fusion events in heterozygous and homozygous CAPS1 KO chromaffin cells, respectively, but found no evidence for an effect of CAPS1 loss on single spike parameters (Figures 4 and 5; Table S2), ruling out a role of CAPS1 in fusion or fusion pore expansion.

CAPS1 and CAPS2 are highly homologous and have very similar activities in in vitro assays of LCDV secre-

tion from PC12 cells (Speidel et al., 2003), but in vivo, CAPS1 and CAPS2 are developmentally and spatially segregated in chromaffin cells (Speidel et al., 2003). This leads to an almost perfect inverse correlation between CAPS1 and CAPS2 levels such that coexpression occurs only in a rather brief time window (Figure 3A and Figure S1). Moreover, CAPS1 and CAPS2 appear to be present on two different types of LDCVs in chromaffin cells (Figure 3B), indicating a complementary function and excluding the possibility that the CAPS1 KO phenotype observed here is influenced by the redundant activity of CAPS2.

How and why CAPS1 and CAPS2 are differentially regulated during development and spatially segregated into two different vesicle populations in chromaffin cells remains unknown. It is possible that they bind to and sort vesicles with different cargo (e.g., ADR versus NA) or that they represent LDCVs of different biogenic origin.

Experimental Procedures

In this study, wt, heterozygous (+/−) CAPS1 KO, or homozygous (−/−) CAPS1 KO mice from E19 and P30 were used for all experiments.

Stem Cell Experiments
CAPS1 KO mice were generated by homologous recombination in embryonic stem cells as described (Augustin et al., 1999; Thomas and Capecchi, 1987). For the CAPS1 targeting vector (Figure 1A), the genomic clone pBS-CAPS-8.2 containing two coding exons (homologous to bp 1026–1258 and bp 1259–1380 of rat CAPS1 cDNA; GenBank accession number U16802) was used. In the targeting vector, the 3′ exon (bp 1259–1380) representing residues 399–439 of CAPS1 protein was replaced by a neomycin resistance cassette. Following electroporation and selection, recombinant stem cell clones were analyzed by Southern blotting after digestion of genomic DNA with XbaI. Four recombinant clones were identified, one of which was injected into mouse blastocysts to obtain highly chimeric mice that transmitted the mutation through the germline. To verify germline transmission, Southern blots with genomic DNA and Western blots with brain extracts were performed. Routine genotyping was performed by PCR.

Western Blotting
Brains and adrenal glands from E19 and P30 mice of the different genotypes were prepared and analyzed as described (Speidel et al., 2003). The following antibodies were used for Western blots: polyclonal rabbit antisera to CAPS1 (Speidel et al., 2003), CAPS2 (Speidel et al., 2003), Munc18-1 (Synaptic Systems), Secretogranin (H.H. Gerdes, Heidelberg, Germany), Chromogranin A (WE-14) (Hamelink et al., 2002), VMAT1 (Weihe et al., 1994), VMAT2 (Weihe and Eiden, 2000), V_0 ATPase (Synaptic Systems), and monoclonal antibodies to Synaptotagmin 1 and Syntaxin 1 (Synaptic Systems) and Actin (Sigma). For quantification of Western blot signals obtained in E19 adrenal gland samples, blots were incubated with a HRP-coupled secondary antibody, and immunoreactive proteins were visualized with enhanced chemiluminescence (Amersham Biosciences). Chromogranin A and Actin were used as loading controls. Signal intensity was determined densitometrically (Agfa-Photo-Look 3.00.07 and TINA 2.0). For the determination of the relative antibody affinity of anti-CAPS1 and anti-CAPS2 antibodies, exactly homologous sequence stretches including the respective regions that had been used as antigens (rat CAPS1, aa 218–390; mouse CAPS2, aa 160–333) (Speidel et al., 2003) were expressed as His-tagged proteins in bacteria, purified on Ni-NTA-beads, and loaded onto SDS-PAGE gels. Coomassie-stained bands were quantified with the Odyssey imaging system (LI-COR) using bovine serum albumin as standard. Defined amounts of fusion proteins (0.4–30 ng) were then analyzed by Western blots using CAPS1 and CAPS2 an-

tisera, respectively. Ratios of signal intensities to loaded protein were compared after densitometric analysis.

Morphological Methods
Cresyl violet staining (Sigma) was performed on frozen sections of E19 and P30 brains and adrenal glands according to standard procedures. Images were captured with a Zeiss Axiophot microscope (Zeiss) and a Camedia C-3030 Zoom digital camera (Olympus). Immunocytochemistry of adrenal glands was performed as described using affinity-purified polyclonal antibodies to CAPS1 and CAPS2 (Speidel et al., 2003). Images were captured with an Axiovert 200 LSM510 laser scanning microscope (Zeiss) and analyzed with the LSM510 software. Immunohistochemical analyses of adrenals with sheep anti-tyrosine hydroxylase (Chemicon), anti-VMAT1, and anti-VMAT2 antibodies, which recognize mouse proteins, were performed as described using Bouin Hollande fixation (Weihe and Eiden, 2000; Weihe et al., 1994). Images were captured with an Axiovert 200 LSM510 laser scanning microscope (Zeiss) and analyzed with the LSM510 software. Glyoxylic acid staining was performed according to De la Torre (1980). Ultrastructural analyses on adrenals from perfused P30 and E19 mice were performed according to standard procedures (Augustin et al., 2001) using a LEO 912AB transmission electron microscope (Zeiss). Images were captured with a ProScan CCD camera and analyzed with the Analysis version 3.2 software (Soft Imaging System). Isolated chromaffin cells were fixed with 4% paraformaldehyde in PBS and incubated with a monoclonal CAPS1 antibody (BD Laboratories) and a polyclonal anti-CAPS2 antibody (Speidel et al., 2003). Following incubation with secondary antibodies (Alexa 488 goat anti-mouse for CAPS1 and Alexa 555 goat anti-rabbit for CAPS2) and several washes, confocal images were taken through the middle of the cell. Images were background subtracted, and a linear unmixing was performed.

Quantitative Analysis of Catecholamines and Catechols
Adrenals were removed, transferred to 100 µl 0.1 M perchloric acid, and frozen in liquid nitrogen. Samples were sonicated, and an aliquot of 50 µl was assayed for protein concentration. After centrifugation at 10,000 g for 10 min, 20 µl of the clear supernatant were injected into an HPLC, coupled with two electrochemical detectors as previously reported (Fornai et al., 2003), to measure levels of catecholamines and catechols.

Chromaffin Cell Preparation and Infection
Mouse embryos at E19 were obtained by caesarean section of pregnant females from timed matings. Adrenal glands were removed, and slices of 80–100 µm thickness were prepared as described previously (Moser and Neher, 1997). Slices were used for 4–6 hr starting shortly after cutting. The preparation of isolated chromaffin cells followed standard procedures previously published (Ashery et al., 2000). For the rescue experiment in Figure 7G, isolated chromaffin cells were infected with 50 µl of activated pSFV1-CAPS1-GFP as described (Ashery et al., 1999).

Patch-Clamp Analyses and Amperometry
Conventional whole-cell recordings were performed with 3–4 MΩ pipettes and an EPC-9 patch-clamp amplifier together with Pulse software (HEKA). The solutions for adrenal slices were as described (Voets, 2000). For measurements from isolated chromaffin cells, the extracellular solution contained 146 mM NaCl, 2.4 mM KCl, 10 mM HEPES, 1.2 mM $MgCl_2$, 2.5 mM $CaCl_2$, 10 mM glucose, and 10 mM $NaHCO_3$ (pH 7.4). The intracellular solution for isolated cells contained 100 mM Cs-aspartate, 10 mM NaCl, 2 mM Mg-ATP, 0.2 mM Na_2-GTP, 40 mM Cs-HEPES, 5 mM nitrophenyl-EGTA (NP-EGTA), 4 mM $CaCl_2$, 0.4 mM Furaptra, and 0.4 mM Fura-4F (pH 7.2). Capacitance measurements were performed using the Lindau-Neher technique implemented as the "sine + dc" mode of the "software lock-in" extension of Pulse software. A 1 kHz, 70 mV peak-to-peak sinusoid stimulus was applied about a DC holding potential of −80 mV. Amperometry recordings on isolated chromaffin cells were performed as published (Bruns et al., 2000). The duration of the foot signal (Figures 4F and 5F and Table S2) was determined as follows: the start of the foot signal was defined as the time point

where the current amplitude exceeded two times the standard deviation of the average baseline noise. Its end was defined as the inflection point between the slowly increasing foot signal and the more rapidly increasing spike current. All experiments were performed at room temperature. Measurements of $[Ca^{2+}]_i$ and photolysis of caged Ca^{2+} was performed as described (Voets, 2000).

TIRFM

TIRFM on wt and homozygous CAPS1 KO chromaffin cells was performed 8–12 hr after infection with a Neuropeptide Y-Venus (NPY-Venus) construct. A single-line (488 nm) laser beam was coupled into the epifluorescence port of an Olympus IX70 microscope equipped with a TIRF condenser (TILL Photonics) and focused off axis to the most peripheral position on the back focal plane of a 1.45 NA 60× oil immersion objective to generate an evanescent field with a penetration depth of about 200 nm. Images were collected at 3 Hz with a Micromax 512 BFT CCD camera (Princeton Instruments) and analyzed using MetaMorph v5.05 (Universal Imaging Corporation). The "total number of vesicles per frame" was counted using the automated object analyzing module of Meta-Morph, and the secretion events were visually detected as a sudden increase in fluorescent intensity followed by a sharp decrease of fluorescence corresponding to the release of NPY-Venus from the vesicle. The increase of the fluorescence intensity corresponded to the dequenching of the fluorophore.

Supplemental Data

The Supplemental Data include two supplemental figures and two supplemental tables and can be found with this article online at http://www.neuron.org/cgi/content/full/46/1/75/DC1/.

References

Ahnert-Hilger, G., Holtje, M., Pahner, I., Winter, S., and Brunk, I. (2003). Regulation of vesicular neurotransmitter transporters. Rev. Physiol. Biochem. Pharmacol. *150*, 140–160.

Ann, K., Kowalchyk, J.A., Loyet, K.M., and Martin, T.F. (1997). Novel Ca^{2+}-binding protein (CAPS) related to UNC-31 required for Ca^{2+}-activated exocytosis. J. Biol. Chem. *272*, 19637–19640.

Ashery, U., Betz, A., Xu, T., Brose, N., and Rettig, J. (1999). An efficient method for infection of adrenal chromaffin cells using the Semliki Forest virus gene expression system. Eur. J. Cell Biol. *78*, 525–532.

Ashery, U., Varoqueaux, F., Voets, T., Betz, A., Thakur, P., Koch, H., Neher, E., Brose, N., and Rettig, J. (2000). Munc13-1 acts as a priming factor for large dense-core vesicles in bovine chromaffin cells. EMBO J. *19*, 3586–3596.

Augustin, I., Betz, A., Herrmann, C., Jo, T., and Brose, N. (1999). Differential expression of two novel Munc13 proteins in rat brain. Biochem. J. *337*, 363–371.

Augustin, I., Korte, S., Rickmann, M., Kretzschmar, H.A., Südhof, T.C., Herms, J.W., and Brose, N. (2001). The cerebellum-specific Munc13 isoform Munc13-3 regulates cerebellar synaptic transmission and motor learning in mice. J. Neurosci. *21*, 10–17.

Avery, L., Bargmann, C.I., and Horvitz, H.R. (1993). The Caenorhabditis elegans unc-31 gene affects multiple nervous system-controlled functions. Genetics *134*, 455–464.

Becherer, U., Moser, T., Stühmer, W., and Oheim, M. (2003). Calcium regulates exocytosis at the level of single vesicles. Nat. Neurosci. *6*, 846–853.

Berwin, B., Floor, E., and Martin, T.F. (1998). CAPS (mammalian UNC-31) protein localizes to membranes involved in dense-core vesicle exocytosis. Neuron *21*, 137–145.

Bruns, D., and Jahn, R. (1995). Real-time measurement of transmitter release from single synaptic vesicles. Nature *377*, 62–65.

Bruns, D., Riedel, D., Klingauf, J., and Jahn, R. (2000). Quantal release of serotonin. Neuron *28*, 205–220.

Burgoyne, R.D., and Morgan, A. (2003). Secretory granule exocytosis. Physiol. Rev. *83*, 581–632.

Cisternas, F.A., Vincent, J.B., Scherer, S.W., and Ray, P.N. (2003). Cloning and characterization of human CADPS and CADPS2, new members of the Ca^{2+}-dependent activator for secretion protein family. Genomics *81*, 279–291.

De la Torre, J.C. (1980). An improved approach to histofluorescence using the SPG method for tissue monoamines. J. Neurosci. Methods *3*, 1–5.

Elhamdani, A., Martin, T.F., Kowalchyk, J.A., and Artalejo, C.R. (1999). Ca^{2+}-dependent activator protein for secretion is critical for the fusion of dense-core vesicles with the membrane in calf adrenal chromaffin cells. J. Neurosci. *19*, 7375–7383.

Erickson, J.D., Schafer, M.K., Bonner, T.I., Eiden, L.E., and Weihe, E. (1996). Distinct pharmacological properties and distribution in neurons and endocrine cells of two isoforms of the human vesicular monoamine transporter. Proc. Natl. Acad. Sci. USA *93*, 5166–5171.

Fornai, F., Lenzi, P., Gesi, M., Ferrucci, M., Lazzeri, G., Busceti, C.L., Ruffoli, R., Soldani, P., Ruggieri, S., Alessandri, M.G., and Paparelli, A. (2003). Fine structure and biochemical mechanisms underlying nigrostriatal inclusions and cell death after proteasome inhibition. J. Neurosci. *23*, 8955–8966.

Gong, L.W., Hafez, I., Alvarez de Toledo, G., and Lindau, M. (2003). Secretory vesicles membrane area is regulated in tandem with quantal size in chromaffin cells. J. Neurosci. *23*, 7917–7921.

Grishanin, R.N., Klenchin, V.A., Loyet, K.M., Kowalchyk, J.A., Ann, K., and Martin, T.F. (2002). Membrane association domains in Ca^{2+}-dependent activator protein for secretion mediate plasma membrane and dense-core vesicle binding required for Ca^{2+}-dependent exocytosis. J. Biol. Chem. *277*, 22025–22034.

Hamelink, C., Tjurmina, O., Damadzic, R., Young, W.S., Weihe, E., Lee, H.W., and Eiden, L.E. (2002). Pituitary adenylate cyclase-activating polypeptide is a sympathoadrenal neurotransmitter involved in catecholamine regulation and glucohomeostasis. Proc. Natl. Acad. Sci. USA *99*, 461–466.

Hay, J.C., and Martin, T.F. (1992). Resolution of regulated secretion into sequential MgATP-dependent and calcium-dependent stages mediated by distinct cytosolic proteins. J. Cell Biol. *119*, 139–151.

Henry, J.P., Sagne, C., Bedet, C., and Gasnier, B. (1998). The vesicular monoamine transporter: from chromaffin granule to brain. Neurochem. Int. *32*, 227–246.

Iwasa, K., Oomori, Y., and Tanaka, H. (1999). Acetylcholinesterase activity, and neurofilament protein, and catecholamine synthesizing enzymes immunoreactivities in the mouse adrenal gland during postnatal development. J. Vet. Med. Sci. *61*, 621–629.

Jahn, R., Lang, T., and Südhof, T.C. (2003). Membrane fusion. Cell *112*, 519–533.

Markoglou, N., and Wainer, I.W. (2001). Synthesis and characterization of immobilized dopamine β-hydroxylase in membrane-bound and solubilized formats. J. Biochem. Biophys. Methods *48*, 61–75.

Moser, T., and Neher, E. (1997). Rapid exocytosis in single chromaffin cells recorded from mouse adrenal slices. J. Neurosci. *17*, 2314–2323.

Mosharov, E.V., Gong, L.W., Khanna, B., Sulzer, D., and Lindau, M. (2003). Intracellular patch electrochemistry: regulation of cytosolic catecholamines in chromaffin cells. J. Neurosci. *23*, 5835–5845.

Pahner, I., Holtje, M., Winter, S., Nurnberg, B., Ottersen, O.P., and Ahnert-Hilger, G. (2002). Subunit composition and functional properties of G-protein heterotrimers on rat chromaffin granules. Eur. J. Cell Biol. *81*, 449–456.

Parsons, S.M. (2000). Transport mechanisms in acetylcholine and monoamine storage. FASEB J. *14*, 2423–2434.

Peaston, R.T., and Weinkove, C. (2004). Measurement of catecholamines and their metabolites. Ann. Clin. Biochem. *41*, 17–38.

Renden, R., Berwin, B., Davis, W., Ann, K., Chin, C., Kreber, R., Ganetzky, B., Martin, T.F., and Broadie, K. (2001). *Drosophila* CAPS is an essential gene that regulates dense-core vesicle release and synaptic vesicle fusion. Neuron *31*, 421–437.

Rettig, J., and Neher, E. (2002). Emerging roles of presynaptic proteins in Ca^{++}-triggered exocytosis. Science *298*, 781–785.

Rupnik, M., Kreft, M., Sikdar, S.K., Grilc, S., Romih, R., Zupancic, G., Martin, T.F., and Zorec, R. (2000). Rapid regulated dense-core vesicle exocytosis requires the CAPS protein. Proc. Natl. Acad. Sci. USA *97*, 5627–5632.

Schonn, J.S., Desnos, C., Henry, J.P., and Darchen, F. (2003). Transmitter uptake and release in PC12 cells overexpressing plasma membrane monoamine transporters. J. Neurochem. *84*, 669–677.

Schuldiner, S. (1994). A molecular glimpse of vesicular monoamine transporters. J. Neurochem. *62*, 2067–2078.

Speidel, D., Varoqueaux, F., Enk, C., Nojiri, M., Grishanin, R.N., Martin, T.F., Hofmann, K., Brose, N., and Reim, K. (2003). A family of Ca^{2+}-dependent activator proteins for secretion: comparative analysis of structure, expression, localization, and function. J. Biol. Chem. *278*, 52802–52809.

Steyer, J.A., Horstmann, H., and Almers, W. (1997). Transport, docking and exocytosis of single secretory granules in live chromaffin cells. Nature *388*, 474–478.

Südhof, T.C. (1995). The synaptic vesicle cycle: a cascade of protein-protein interactions. Nature *375*, 645–653.

Tabares, L., Ales, E., Lindau, M., and Alvarez de Toledo, G. (2001). Exocytosis of catecholamine (CA)-containing and CA-free granules in chromaffin cells. J. Biol. Chem. *276*, 39974–39979.

Tandon, A., Bannykh, S., Kowalchyk, J.A., Banerjee, A., Martin, T.F., and Balch, W.E. (1998). Differential regulation of exocytosis by calcium and CAPS in semi-intact synaptosomes. Neuron *21*, 147–154.

Thomas, K.R., and Capecchi, M.R. (1987). Site-directed mutagenesis by gene targeting in mouse embryo-derived stem cells. Cell *51*, 503–512.

Voets, T. (2000). Dissection of three Ca^{2+}-dependent steps leading to secretion in chromaffin cells from mouse adrenal slices. Neuron *28*, 537–545.

Voets, T., Neher, E., and Moser, T. (1999). Mechanisms underlying phasic and sustained secretion in chromaffin cells from mouse adrenal slices. Neuron *23*, 607–615.

Walent, J.H., Porter, B.W., and Martin, T.F. (1992). A novel 145 kd brain cytosolic protein reconstitutes Ca^{2+}-regulated secretion in permeable neuroendocrine cells. Cell *70*, 765–775.

Wang, Y.M., Gainetdinov, R.R., Fumagalli, F., Xu, F., Jones, S.R., Bock, C.B., Miller, G.W., Wightman, R.M., and Caron, M.G. (1997). Knockout of the vesicular monoamine transporter 2 gene results in neonatal death and supersensitivity to cocaine and amphetamine. Neuron *19*, 1285–1296.

Wassenberg, J.J., and Martin, T.F. (2002). Role of CAPS in dense-core vesicle exocytosis. Ann. N Y Acad. Sci. *971*, 201–209.

Weihe, E., and Eiden, L.E. (2000). Chemical neuroanatomy of the vesicular amine transporters. FASEB J. *14*, 2435–2449.

Weihe, E., Schafer, M.K., Erickson, J.D., and Eiden, L.E. (1994). Localization of vesicular monoamine transporter isoforms (VMAT1 and VMAT2) to endocrine cells and neurons in rat. J. Mol. Neurosci. *5*, 149–164.